AMERICAN SOCIETY FOR MICROBIOLOGY | Molecular and Cellular Biology®

RESEARCH ARTICLE

Import of TAT-Conjugated Propionyl Coenzyme A Carboxylase Using Models of Propionic Acidemia

Renata Collard,[a] Tomas Majtan,[a] Insun Park,[a] Jan P. Kraus[a]

[a]Department of Pediatrics, University of Colorado School of Medicine, Aurora, Colorado, USA

ABSTRACT Propionic acidemia is caused by a deficiency of the enzyme propionyl coenzyme A carboxylase (PCC) located in the mitochondrial matrix. Cell-penetrating peptides, including transactivator of transcription (TAT), offer a potential to deliver a cargo into the mitochondrion. Here, we investigated the delivery of an $\alpha_6\beta_6$ PCC enzyme into mitochondria using the HIV TAT peptide at several levels: into isolated mitochondria, in patient fibroblast cells, and in a mouse model. Results from Western blots and enzyme activity assays confirmed the import of TAT-PCC into mitochondria, as well as into patient fibroblasts, where the colocalization of imported TAT-PCC and mitochondria was also confirmed by confocal fluorescence microscopy. Furthermore, a single-dose intraperitoneal injection into PCC-deficient mice decreased the propionylcarnitine/acetylcarnitine (C3/C2) ratio toward the normal level. These results show that a cell-penetrating peptide can deliver active multimeric enzyme into mitochondria *in vitro*, *in situ*, and *in vivo* and push the size limit of intracellular delivery achieved so far. Our results are promising for other mitochondrion-specific deficiencies.

KEYWORDS mitochondria, cell-penetrating peptide, enzyme replacement, organic acidemia

Inherited metabolic disorders represent a therapeutic challenge and, in recent years, there has been an increased search for new-era treatments for metabolic disorders, such as enzyme replacement therapy (ERT) or gene therapy (1). Propionic acidemia (PA) belongs to this category, since it is an autosomal recessive disorder in which a defective form of the enzyme propionyl coenzyme A (propionyl-CoA) carboxylase (PCC) results in the accumulation of propionic acid, propionyl-CoA, methylcitrate, propionylcarnitine, and 3-hydroxypropionate in body fluids.

PCC catalyzes the conversion of propionyl-CoA to D-methylmalonyl-CoA in the mitochondrial matrix (Fig. 1) (2). The PCC enzyme is an $\alpha_6\beta_6$ heterododecamer of ~780 kDa consisting of two types of subunits, α and β, encoded by two different nuclear genes, designated PCCA and PCCB, respectively. The β-subunits form a central hexameric core decorated on the outside by six noninteracting α-subunits. Biotin, bicarbonate, and ATP have binding sites on the α-subunit, whereas propionyl-CoA binds to the β-subunit.

Previous studies of the human enzyme have indicated that the α-subunit is 72 kDa in size, whereas β-subunit is 54 kDa (3). The crystal structure of bacterial propionyl-CoA carboxylase dodecamer has been solved successfully providing the three-dimensional structure of the enzyme (4).

Propionic acidemia (OMIM 606054) usually presents as a life-threatening metabolic ketoacidosis in the neonatal period with protein intolerance, vomiting, failure to thrive, and lethargy (2). Currently, there is no cure, and the treatment is based on dietary management recommending low protein diet and limiting the intake of propiogenic substrates. In addition, the use of supplements such as L-carnitine is recommended.

Received 14 September 2017 **Returned for modification** 17 October 2017 **Accepted** 9 January 2018

Accepted manuscript posted online 29 January 2018

Citation Collard R, Majtan T, Park I, Kraus JP. 2018. Import of TAT-conjugated propionyl coenzyme A carboxylase using models of propionic acidemia. Mol Cell Biol 38:e00491-17. https://doi.org/10.1128/MCB.00491-17.

Address correspondence to Jan P. Kraus, jan.kraus@ucdenver.edu.

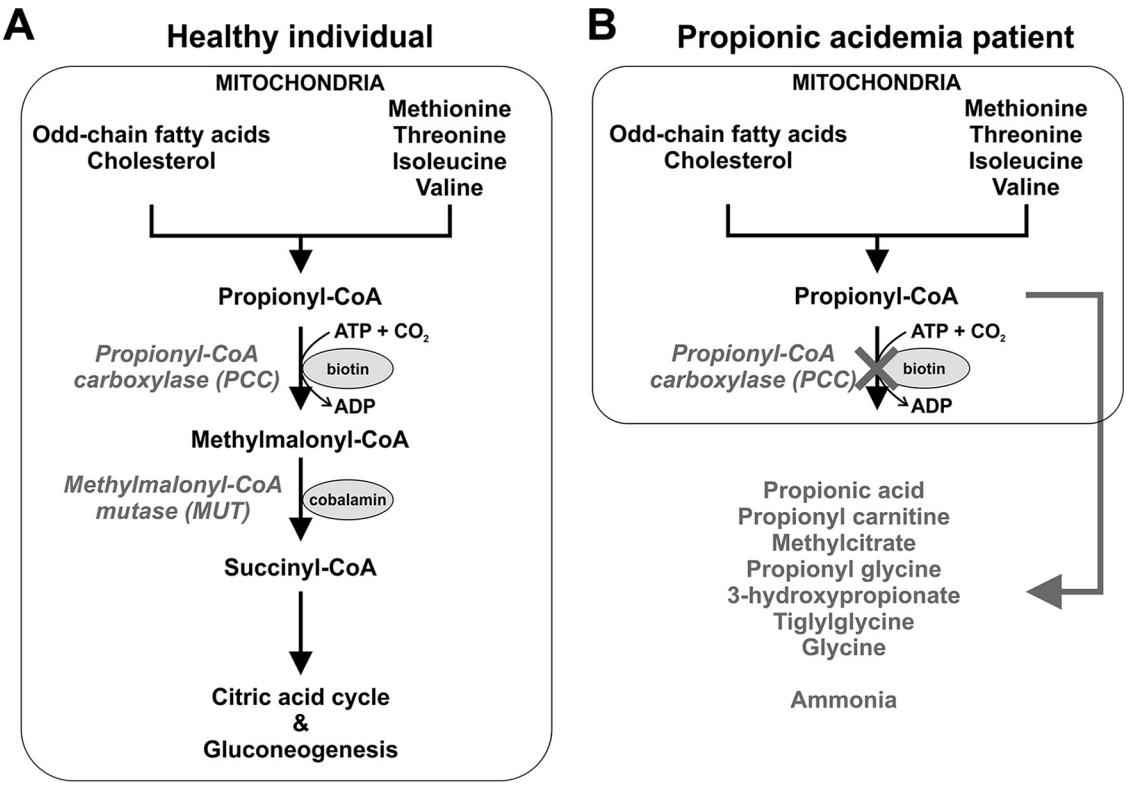

FIG 1 Metabolic impairment in propionic acidemia. (A) PCC catalyzes in the mitochondrial matrix the conversion of propionyl-CoA to D-methylmalonyl-CoA, which enters the Krebs cycle via succinyl-CoA. The sources of propionate include methionine threonine, isoleucine, valine, odd-chain fatty acids, and cholesterol. (B) Deficiency of PCC results in propionic acidemia (PA) with accumulation of propionic acid, propionylcarnitine (C3), methylcitrate, propionylglycine, and 3-hydroxypropionate among other metabolites.

Liver transplantation is being utilized with limited success (5). Thus, ERT would represent a major improvement in treatment of patients if the enzyme or its subunits could be imported into the mitochondrial matrix.

ERT for mitochondrial enzymes requires transport of the cargo through the plasma membrane, as well as through the outer and inner mitochondrial membranes. First, delivery of protein is limited by its ability to penetrate the cell membrane. To overcome this obstacle, the HIV transactivator of transcription (TAT) transduction domain is used most frequently for various types of cargo, not only proteins. TAT was first reported in 1988 (6, 7). The minimal peptide sequence of TAT protein responsible for cellular uptake is 47-YGRKKRRQRRR-57, which contains six arginine and two lysine residues and therefore possesses a high net positive charge at the physiological pH.

Mitochondria are made up of a two-membrane system. While the mitochondrial outer membrane is similar to the plasma membrane in terms of protein/lipid ratio (1:1), there are no proteoglycans present on the surface of mitochondria, although the phospholipid cardiolipin imparts a net negative charge to the membrane. The inner mitochondrial membrane displays a higher protein/lipid ratio (3:1) compared to the plasma and outer mitochondria membranes (8), meaning that the mechanism of import into the mitochondrial matrix space circumvents the difference in membrane composition. Apart from proteins encoded by the mitochondrial genome, most of the mitochondrial proteins need to be delivered into this organelle following their translation on cytoplasmic ribosomes. They are then transported with the help of leader sequences, translocases, and chaperones (9). The leader or the mitochondrial targeting sequence (MTS) is recognized by a receptor in the translocase of the outer membrane. Transport across the mitochondrial membranes requires the concerted action of a number of translocation machineries of Tom complex (translocator outer membrane)

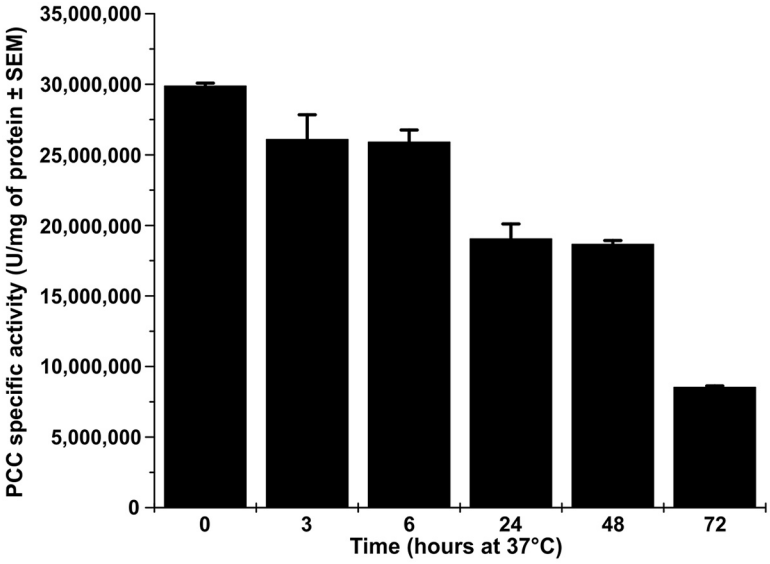

FIG 2 Stability of PCC enzyme in A138T mouse plasma at 37°C. Stability of PCC was evaluated by following the enzymatic activity over time for up to 72 h. PCC was diluted to a final concentration of 0.1 mg/ml in A138T mouse plasma, followed by incubation for the indicated times. The incubation was terminated by mixing 18 μl of the reaction mixture with 2 μl of protease inhibitor cocktail (Sigma; catalog no. 8340) on ice, and the PCC activity was determined. The results are an average of two measurements ± the standard errors of the mean (SEM).

and Tim complex (translocator inner membrane) (10). Soon after a protein arrives in the mitochondrial matrix, a Zn-dependent protease removes its N-terminal MTS (11, 12).

TAT fusion proteins with or without MTS have been used numerous times for protein delivery into mitochondria. The presence of TAT did not negatively affect the biological activity of the cargo proteins (13). The TAT domain with or without the MTS was used to deliver lipoamide dehydrogenase (LAD) to mitochondria in fibroblasts from patients suffering from LAD deficiency. Furthermore, this transduced enzyme appeared to be able to replace the defective enzyme in a large multisubunit complex to restore enzymatic function to near-normal levels. LAD is the third catalytic subunit (E3) of three-component enzyme complex in the mitochondrial matrix (14, 15). Another successful application of the TAT-MTS-protein delivery approach into mitochondria was the replacement of the C6ORF66 assembly factor to restore complex I activity in patient cells (16) or a replacement of frataxin that increased life span and cardiac function in a conditional Friedreich's ataxia mouse model (17). The question how big a protein could actually be imported has never been answered. For our enzyme of interest, PCC, one report was published recently describing mitochondrial import of either single α- or β-subunit using TAT (18). Encouraged by these reports, we tested the import of a biologically active, fully assembled PCC dodecamer, posttranslationally chemically conjugated with TAT.

RESULTS

Stability of PCC in mouse plasma. We were interested in determining what the stability of human recombinant PCC is in mouse plasma at 37°C. As shown in Fig. 2, the enzyme is relatively stable in plasma, with an approximately 40% decrease by 24 h and ~1/3 of its activity still intact by 72 h. This experiment showed that injecting PCC into circulation will not result in its immediate degradation, thus enabling its transport via the bloodstream to target tissues.

Conjugation of TAT peptides to individual PCC subunits. It was important to determine whether the TAT peptide modifies cysteine(s) in the α- or β-subunit or in both subunits. Toward that aim, we conjugated PCC with fluorescein isothiocyanate (FITC)-labeled TAT peptide (Kerafast) to be able to follow the fluorescent label on a

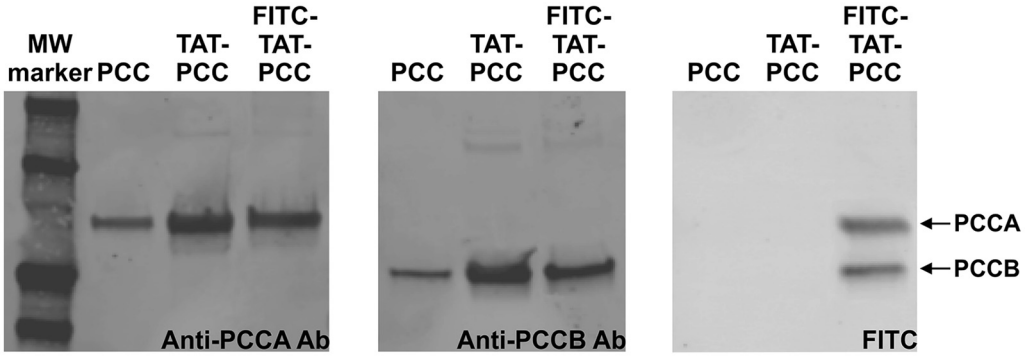

FIG 3 Western blot of PCC conjugation with fluorescent TAT peptide. Purified PCC was conjugated with FITC-labeled TAT peptide at a TAT/PCC molar ratio of 2:1 for 3 h. The unconjugated peptide was removed using a Bio-Spin 6 column (Bio-Rad). The left and middle panels show Typhoon scanning with a red laser at 633 nm for PCC subunit detection with PCC antibodies, followed by secondary antibody labeled with Alexa Fluor 647. The right panel shows direct imaging of FITC-TAT-PCC with a green 532-nm laser for the FITC label.

Western blot using a Typhoon imager (GE Healthcare). Figure 3 shows the results of this conjugation. In Fig. 3 (left panel), we see detection of the PCCA subunits with anti-PCCA antibody, which detects the unmodified PCCA subunit in PCC, as well as the TAT-modified PCCA subunit in both TAT-PCCA and FITC-TAT-PCCA. In the middle panel, a similar result was obtained using anti-PCCB antibody for the PCCB subunit. In Fig. 3 (right panel), we see the results obtained for the same preparations using the fluorescence detection in the Typhoon imager. The unmodified PCC and TAT-PCC are not detected because they do not contain the fluorescent label, while both PCC subunits are detected when the FITC-labeled TAT peptide was used. This experiment clearly shows that each subunit was modified with the TAT peptide; however, the number of targeted cysteines and their sequence positions were not determined.

Trypsin proteolysis of TAT-PCC conjugate. Since trypsin use was planned in all import experiments to digest any nonimported TAT-PCC adsorbed to the outside of the outer mitochondrial membrane to ensure that the mitochondrial lysate represented only PCC that had been imported inside the organelle, the susceptibility of the enzyme to digestion by trypsin was first assessed (Fig. 4). The digestion with trypsin at 1:20 (wt/wt) ratio was performed for 1, 2.5, 5, 30, and 60 min in HMS buffer used for mitochondrial import. The time course of TAT-PCC proteolysis with trypsin in HMS buffer was monitored by visualizing the products of trypsin digestion on SDS–10% PAGE (Fig. 4A) gels, as well as by measuring the PCC activity (Fig. 4B). As a control, trypsin inhibitor was included in a reaction mixture prior to trypsin addition, which resulted in no TAT-PCC degradation and no loss of enzymatic activity, suggesting that the inhibitor efficiently neutralized the protease. On the other hand, incubation of the conjugate with trypsin over a 60-min period resulted in a quick enzyme degradation correlated with a loss of PCC activity. More specifically, 12.8% of the PCC activity remained after 5 min of incubation, and there was no activity or protein left after 30 min of trypsin digestion. Thus, treatment of TAT-PCC with trypsin in a 1:20 (wt/wt) ratio for 5 to 30 min effectively degraded the enzyme, which allowed us to distinguish between the imported and just surface-adsorbed TAT-PCC in subsequent experiments.

Import of TAT-PCC into isolated mitochondria. To get a better understanding how the TAT-PCC delivery functions, we first examined the ability of the conjugate to cross the mitochondrial membrane as a fully functional enzyme (Fig. 5). We incubated 1 μM TAT-PCC with isolated mitochondria from A138T mouse liver at 27°C for 30 min, followed by trypsinization at a 1:20 (wt/wt) ratio for either 5 or 30 min at 37°C. Western blotting confirmed the presence of the delivered enzyme (Fig. 5A). In WT mouse liver mitochondrial lysate, we detected both subunits of the PCC enzyme. On the other hand, the A138T mouse liver mitochondrial lysate did not contain any detectable α-subunit. However, the import of 1 μM TAT-PCC for 30 min into PCC-deficient

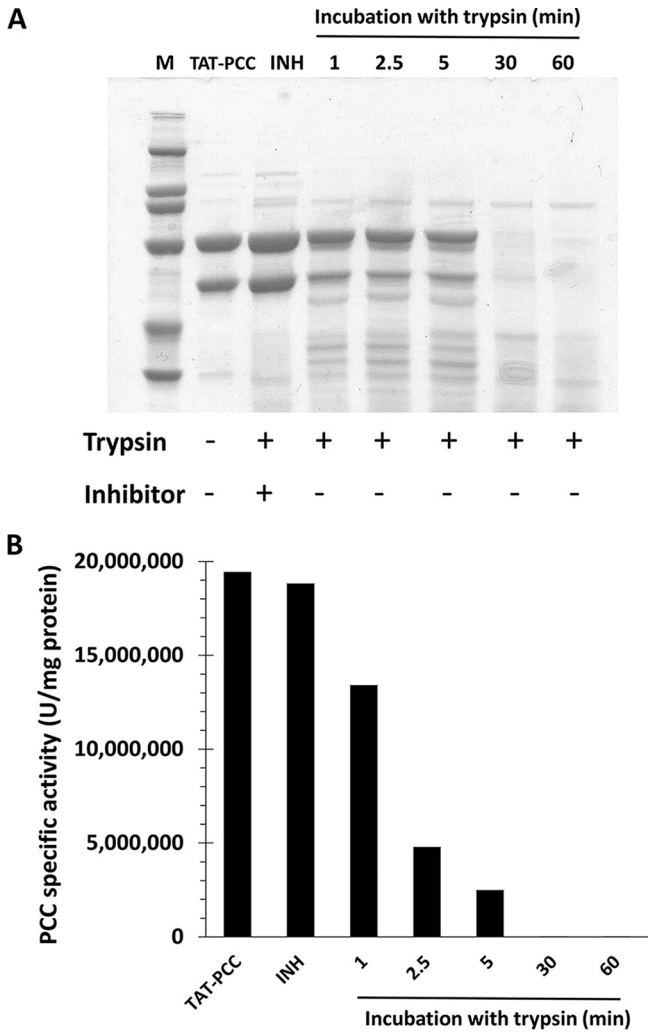

FIG 4 Proteolysis of TAT-PCC. TAT-PCC was incubated with trypsin at a 1:20 (wt/wt) ratio for up to 60 min. At the designated time points, the reaction was stopped by the addition of trypsin inhibitor and samples were analyzed using SDS-PAGE (A) and PCC activity assay (B). Lane M, broad-range SDS-PAGE protein standard (Bio-Rad); lane TAT-PCC, untreated conjugate; lane INH, TAT-PCC proteolyzed with trypsin for 30 min in the presence of a trypsin inhibitor. The samples that follow represent TAT-PCC trypsin proteolysis reactions terminated by the addition of trypsin inhibitor at 1, 2.5, 5, 30, and 60 min.

mitochondria resulted in clear accumulation, and detection of both α- and β-subunits in samples without or with the trypsin treatment clearly indicated importation inside the mitochondria and thus protection from the protease. The PCC activity assays performed on the same samples further document that the presence of trypsin for periods of 5 and 30 min did not degrade mitochondria or the PCC already present inside (Fig. 5B). The activity of liver mitochondrial lysate from A138T mouse was significantly lower at about 8% of WT liver activity. After TAT-PCC importation, the detected PCC activity in the lysates reached the levels observed for WT controls. The trypsin treatment did not substantially affect the activity, suggesting that most of the TAT-PCC was imported and protected inside the mitochondria. Oxygen consumption capability of mitochondria was monitored while performing the import and trypsinization to make sure that mitochondria were intact and functional during the study (Fig. 5C). Measurement of oxygen consumption in isolated mitochondria was performed in a closed chamber for approximately 1 h. When the oxygen was used up, the substrate was added. The chamber was then repeatedly opened and closed to see spikes in respiration of the mitochondria.

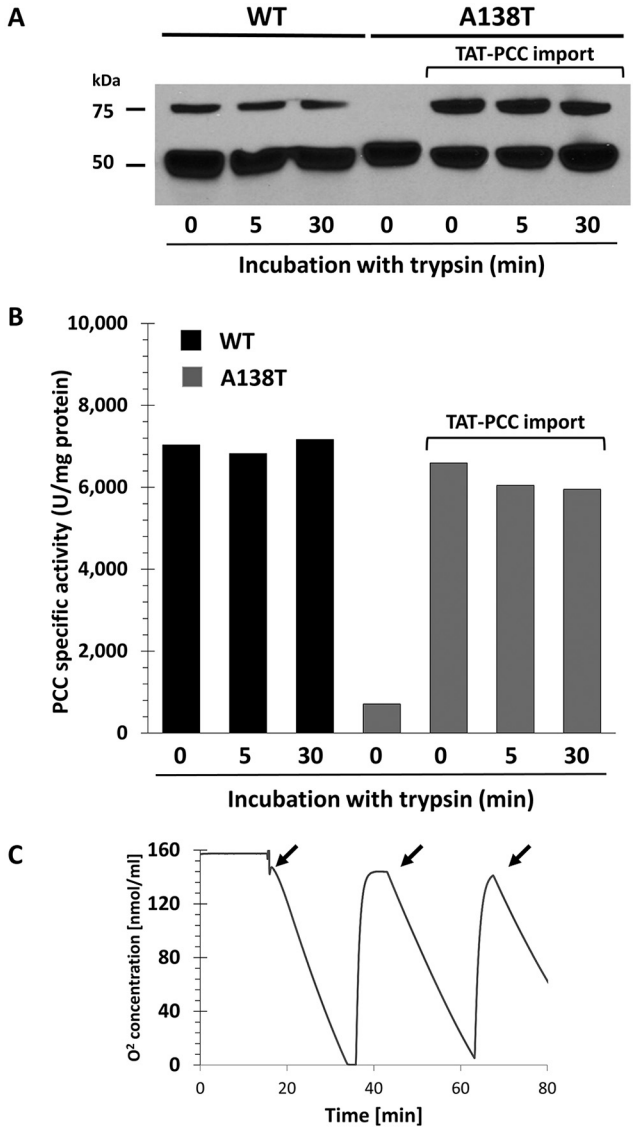

FIG 5 Resistance of mitochondria to trypsin and import of TAT-PCC into mitochondria. (A and B) Western blotting (A) and PCC activity (B) analyses of WT and A138T mitochondrial lysates were performed without or with the import of 1 μM TAT-PCC, respectively, with trypsin treatment for 0, 5, and 30 min. Both panels A and B demonstrate protection of the mitochondrion-imported TAT-PCC from trypsin. (C) The respiration of A138T mitochondria was monitored for 80 min under conditions identical to the import. The arrows indicate additions of the substrate.

In the next step, we investigated the dose-dependent character of the import (Fig. 6). In addition to 1 μM TAT-PCC import into A138T mouse mitochondria, we added two and five times more of the conjugate. As evidenced from Western blotting (Fig. 6A) and the PCC activity plot (Fig. 6B) of the mitochondrial lysates after import, we observed a linear, but not dose-proportional, increase in mitochondrion-imported PCC activity with increasing amounts of TAT-PCC. Specifically, a 1 μM import of TAT-PCC resulted in a 7-fold increase compared to A138T mouse mitochondrial enzyme activity and, at the same time, normalization to the levels of PCC activity measured for WT mitochondria. Import of 2 and 5 μM TAT-PCC further increased PCC activity 13- and 20-fold, respectively, compared to A138T mouse mitochondria. Thus, increased amounts of the conjugate lead to increased importation of TAT-PCC into mitochondria.

Import of TAT-PCC into patient fibroblasts. After the successful studies with isolated A138T liver mouse mitochondria, we examined the TAT-PCC import into

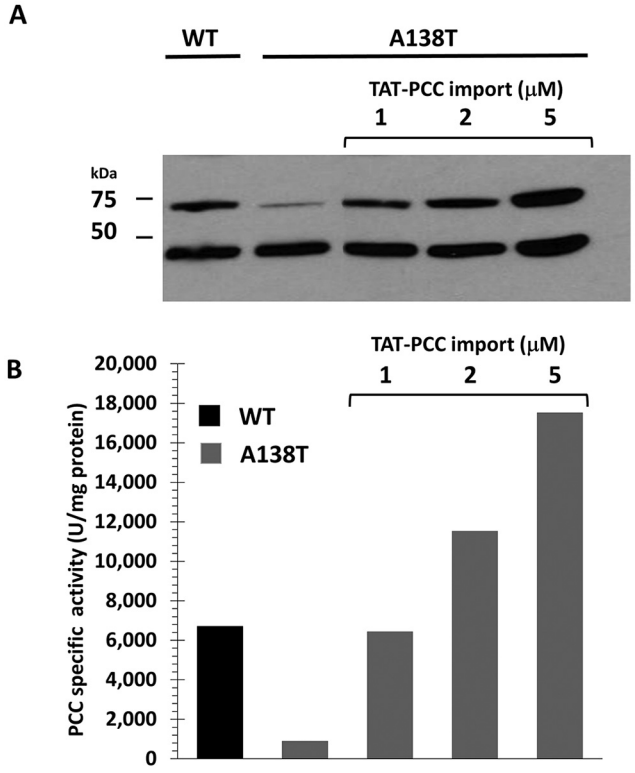

FIG 6 Dose-dependent import of TAT-PCC into A138T mitochondria. After import for 30 min, the mitochondria were treated with trypsin for 30 min, centrifuged, and lysed with lysis buffer. Western blotting (A) and PCC activity (B) analyses of WT and A138T mitochondrial lysates were performed without import as negative and positive controls, respectively, and after the import of 1, 2, and 5 μM TAT-PCC, followed by a 30-min trypsin treatment. Please note that in panel A an empty lane between the A138T lanes without and with 1 μM TAT-PCC import was cut out from the image.

cultured skin fibroblasts from PA patients deficient in either α- or β-subunit. The cells were incubated with 1, 5, or 10 μM TAT-PCC for 1 h, and the PCC activity was then determined in the fibroblast lysates (Fig. 7). Both patient fibroblast extracts had initially $<$3% of the WT control fibroblast activity. The increased amount of TAT-PCC resulted

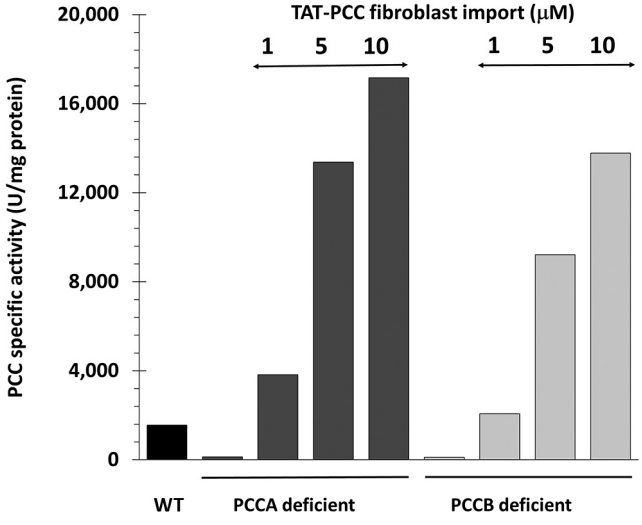

FIG 7 Import of TAT-PCC into PCC-deficient fibroblasts. Both PCCA- and PCCB-deficient cultured patient fibroblasts were incubated with 1, 5, or 10 μM TAT-PCC for 1 h. The resulting PCC activity in lysates was compared to the PCC activity of a WT fibroblast lysate. Note that the first PCCA- and PCCB-deficient lanes in each case are negative controls with no import.

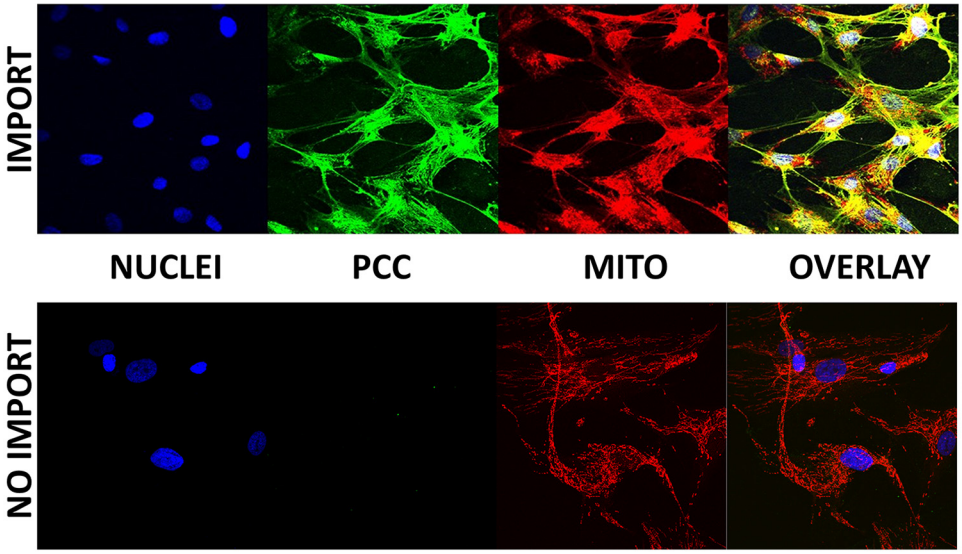

FIG 8 Mitochondrial colocalization of imported TAT-PCC in PCC-deficient fibroblasts. Import of 1 μM TAT-PCC into PCCA-deficient fibroblasts for 1 h at 37°C (top) was compared to that for identical cells with no import (bottom). The live cells were stained with MitoTracker CMXRos (mito). After the cell fixation, staining was performed with anti-PCCA antibody and then with green fluorescent secondary antibody (PCC); DAPI blue fluorescent dye was used to stain the nuclei (nuclei). The "overlay" images illustrate the superimposition of the three preceding images.

in an increased import and thus recovered PCC activity in the fibroblast lysates. The activity at the highest 10 μM TAT-PCC concentration exceeded the WT control activity by 11- and 9-fold for the α- and β-deficient cells, respectively.

Localization of PCC in mitochondria by confocal microscopy. To confirm the presence of the imported TAT-PCC inside mitochondria, we performed immunostaining and confocal microscopy of PCCA-deficient patient fibroblast cells after the import of 1 μM TAT-PCC (Fig. 8). Detection of PCC in cells after import resulted in pan-cellular staining consistent with a cellular delivery of TAT-PCC (Fig. 8, top). More importantly, substantial overlap with the mitochondrion-specific MitoTracker stain suggested successful import of TAT-PCC inside the mitochondria. As a control, the same cells without import of TAT-PCC showed no presence of PCC (Fig. 8, bottom). Taking these results together with the results shown in Fig. 7, we were able to successfully import an active PCC dodecamer conjugated with TAT peptide inside mitochondria of PA patient fibroblasts.

Single-dose i.p. TAT-PCC injection to PCC-deficient mice. After successful TAT-PCC import into PCC-deficient mouse mitochondria and cultured human PA fibroblasts, we studied the ability of TAT-PCC to correct the plasma metabolic imbalance in A138T mice after a single intraperitoneal (i.p.) administration. Figure 9 shows that 4 h after the injection, the C3/C2 ratio decreased significantly compared to phosphate-buffered saline (PBS)-injected positive controls with a maximal effect reached at 9 h postinjection. However, the C3/C2 ratio remained 13-fold higher versus negative controls at the 9-h time point, which was a marked improvement compared to the 40-fold elevation prior to the TAT-PCC injection. Within 24 h postinjection, the C3/C2 ratios of TAT-PCC- and PBS-injected A138T mice were similar and returned to the pretreatment levels.

[^{14}C]propionate fixation in TAT-PCC-treated mice. To obtain further support for a positive impact of the treatment with TAT-PCC, we carried out incorporation of [1-^{14}C]propionate into cellular macromolecules in PCCA deficient fibroblasts as described previously (19–21). As can be seen in Fig. 10, the PCCA-deficient fibroblast cells incorporated only 12% of the WT control. Pretreatment of the cells with TAT-PCC prior to the addition of the [^{14}C]propionate yielded 25% of WT incorporation, a marked improvement but not yet a complete normalization. Nevertheless, the experiment

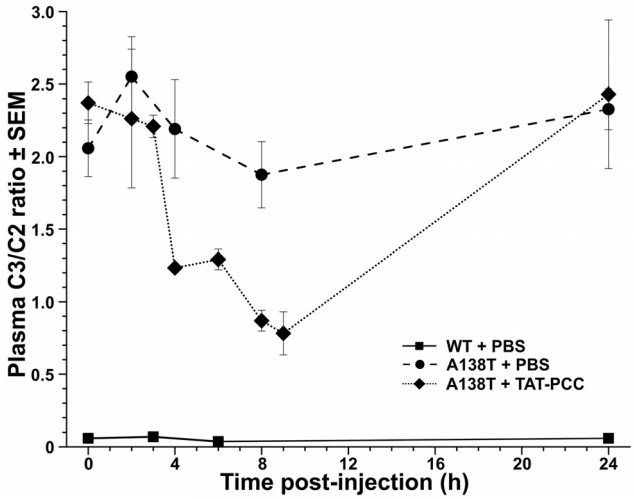

FIG 9 Effect of a single TAT-PCC injection on the plasma C3/C2 ratio in A138T mice. Plasma C3/C2 ratios were monitored over 24 h after a single i.p. injection of 20 mg/kg TAT-PCC ($n = 4$ to 8) or PBS ($n = 4$) in PCC-deficient A138T mice. WT mice injected with PBS served as negative controls ($n = 4$).

provided evidence that the imported PCC reached the inner mitochondrial space, since the PCC-MUT-Krebs cycle is complete only in mitochondria.

DISCUSSION

The TAT protein from human immunodeficiency virus type 1 is a potent viral transactivator that is essential for viral replication. From its discovery, it has been frequently studied for its unique ability to penetrate cell membranes. The TAT dodecapeptide, also used in this study, facilitates cellular uptake of different types of cargo and thus it has been classified into the category of cell penetration peptides. The exact mechanism how TAT-protein complex enters the cells or mitochondria is not fully understood (22, 23). Previous reports have studied the TAT-mediated protein transduction across the plasma membrane of cells, and they have strongly implicated endocy-

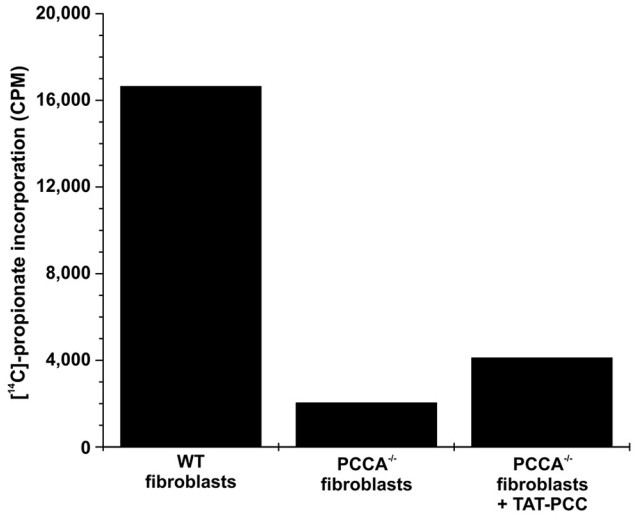

FIG 10 Incorporation of [^{14}C]propionate into WT and PCCA-deficient fibroblasts with or without TAT-PCC import. Fibroblasts were grown to 80% confluence in a six-well plate. Import of 5 μM TAT-PCC or incubation with PBS was performed for 1 h in 37°C as described in Fig. 7. Subsequently, fibroblasts were incubated for 18 h in MEM supplemented with 15% fetal bovine serum (Fetal Clone III) and 100 μM [1-^{14}C]propionate (MD Biochemical), diluted with unlabeled sodium propionate to give a final specific activity of 10 μCi/μmol. The radioactivity incorporated in the precipitate was determined by liquid scintillation counting.

tosis as the mechanism for TAT transduction (24). It was shown, however, in earlier studies that TAT will transduce a protein cargo into mitochondria which are not known to employ any endocytic mechanism (15, 25). Previously, it was suggested that the conjugate of TAT with protein lacking MTS would cross the mitochondrial membrane (13); however, it may not be retained inside mitochondria, but no supportive data were available to confirm such a hypothesis.

To better understand the mechanisms that allows TAT-mediated protein to transduce into mitochondria, one study tested the hypothesis that TAT transduction could be blocked using endocytosis inhibitors. In contrast to TAT transduction across the cell membrane, they found that TAT transduction into mitochondria was not inhibited by compounds known to block endocytosis, thus confirming the TAT-mediated transduction and suggesting an alternative endocytosis-independent mechanism. Surprisingly, compounds known to inhibit endocytosis via blocking the function of sodium channels, such as amiloride, markedly increased TAT transduction into mitochondria, thus Rayapureddi et al. (25) suggested that sodium channels play a major role in mediating TAT protein transport into mitochondria. It was also confirmed that TAT transduction into the mitochondrial matrix occurs via an energy-independent pathway (25). Bacteria, which mitochondria are often compared to, do not perform endocytosis. However, one report showed that a peptidoglycan-less bacterium has indeed a mechanism similar to endocytosis (26).

TAT-mediated import of a whole protein across plasma membrane into mitochondria has been reported multiple times (14). There were attempts to carry out the import with or without the MTS. TAT fusion with malate-dehydrogenase both with and without MTS was shown to traverse mitochondrial membranes; however, it did not remain there if MTS was not used because TAT could not be removed using the MTS cleavage site. Furthermore, this TAT fusion protein was able to cross the placenta, where it was detectable in both fetal and newborn mouse pups (13). The lipoamide dehydrogenase (LAD; also known as E3) subunit was fused with TAT peptide and could rapidly cross the membranes and be delivered into isolated mitochondria. Both TAT-LAD and TAT-MTS-LAD tested positive, although the import without MTS was described as slightly less efficient. The import of TAT-MTS-LAD into patient cells restored LAD activity to normal values (15). Also, TAT-MTS-LAD was successfully delivered into tissues of LAD-deficient mice (27). A successful delivery of TAT-MTS-coupled mitochondrial enzyme into patient cells was also reported for the NAD dehydrogenase complex I assembly factor (NDUFAF4). Mitochondrial complex I deficiency is a disorder caused by mutations in NDUFAF4. A recombinant protein containing the TAT-MTS-NDUFAF4 WT was efficiently taken up by patient-derived NDUFAF4-deficient cells, resulting in a significant increase in complex I activity and improved mitochondrial function (16). Another inherited mitochondrial disorder with no available treatment is Friedrich's ataxia. Recently, Vyas et al. reported efforts to develop a TAT-MTS-frataxin enzyme replacement therapy with encouraging results in disease model mice (17).

PA is a devastating disease with only dietary management treatment. ERT for PA or for any mitochondrial disease would constitute an amazing achievement. The use of ERT has been studied in various metabolic enzyme deficiencies, such as Gaucher's, Hurler's, Fabry's, Pompe's, homocystinuria, PKU, glycogen storage disease type II, and mucopolysaccharidosis I and VI, and in Maroteaux-Lamy syndrome to reverse the pathogenesis of the chief clinical manifestations of these diseases (28–38). Although ERT for mitochondrial disorders is significantly more challenging due to the need for delivery inside an organelle, its application to replace a particular activity of an enzyme is becoming a potentially attractive therapeutic approach in the treatment of enzyme deficiency disorders.

A recent study on an ERT for PA reported on the importation of individual α- and β-subunits with or without MTS (18). These researchers had uncertain success importing of TAT-MTS-PCCA and PCCB-MTS-TAT into PA patient lymphoblasts. Western blotting and a PCC activity assay were used to prove the presence of each imported subunit in the deficient lymphoblasts, although the amounts detected by Western blotting did

not correlate with the activity measurements. Moreover, confocal microscopy showed that the imported constructs into HeLa cells accumulated mostly on the outer edge of the cells and formed clumps, likely due to protein precipitation mentioned by the authors as the major problem during preparation of the constructs. We, too, prepared similar constructs for the expression and import of individual PCC subunits with or without MTS, TAT, and a 6×His purification tag. However, these constructs were mostly completely insoluble, and all attempts to solubilize, further purify, and refold them to make them compatible with the biological systems have failed. Coexpression of α- and β-subunits N-terminally tagged with TAT-MTS sequence also yielded insoluble and inactive protein (data not shown). The only successful approach to obtain soluble TAT-PCC conjugate is described here and included the expression of the native PCC dodecamer in the presence of GroES/EL, the purification of the enzyme to homogeneity (39), and subsequent chemical conjugation with the TAT polypeptide.

To unequivocally demonstrate the cellular import and mitochondrial localization of our TAT-PCC, we first established conditions for quantitative proteolytic removal of all the remaining, nonimported TAT-PCC. We identified such conditions and used them with mitochondria (Fig. 4 and 5). For import of TAT-PCC into fibroblasts, we have employed the standard trypsin treatment (0.25% [2.5 mg/ml] trypsin in PBS for 5 min) to detach the cells from the flask. This protease concentration was 400-fold greater than the one shown to completely degrade PCC (Fig. 4). In addition, we demonstrated that mitochondria are resistant to such treatment and thus protect any protein located inside, including imported TAT-PCC (Fig. 5). We also showed that the import of the TAT-PCC conjugate into mitochondria, as well as patient fibroblasts, was dose dependent, although not proportional (Fig. 6 and 7). Confocal microscopy showed colocalization of imported TAT-PCC with mitochondria, thus confirming that TAT-PCC was delivered inside the mitochondria of intact patient fibroblasts (Fig. 8). A remarkable aspect of our reported protein import that should be emphasized is the size of the cargo. The native PCC dodecamer of ~780 kDa was imported into both the isolated PCC-deficient mouse liver mitochondria and the patient fibroblasts. It has been reported that the native PCC has dimensions of 155 Å by 155 Å by 170 Å (4). Until now, the largest reported size of cargo successfully delivered into cells with the help of TAT was TAT-MTS-LAD (58.1 kDa) (15). The A138T mouse model of PA accumulates propionylcarnitine in plasma; hence, it has a substantially elevated the C3/C2 ratio (Fig. 9). The single i.p. injection of TAT-PCC to A138T mice substantially decreased, although it did not normalize the ratio. This encouraging result will be investigated in depth in future experiments. It should be noted, however, that the import of TAT-PCC is an inefficient process at this time since less than 1% of the input TAT-PCC is found in the mitochondria. More efficient mitochondria targeting peptides will be used in future experiments, followed by removal of the peptide to prevent export back to cytoplasm.

Finally, incorporation of [^{14}C]propionate into cellular macromolecules in WT and PCCA-deficient fibroblasts after treatment of the cells with TAT-PCC (Fig. 10) lent further support to the notion that import of TAT-PCC partially restores the pathway between the PCC and the Krebs cycle in the mitochondrion.

In conclusion, our experiments demonstrated that it is possible to import a very large cargo into mitochondria. This approach may offer a new avenue for treating mitochondrial enzyme deficiencies by ERT.

MATERIALS AND METHODS

Preparation of recombinant human TAT-PCC enzyme from *Escherichia coli*. The expression and purification of recombinant human PCC from *E. coli* was carried out essentially as described previously (39, 43). Briefly, *E. coli* SE1(DE3) cells carrying ampicillin-resistant PCC expression vector pETDS1-PCCAB and chloramphenicol-resistant GroEL/ES expression plasmid pGro7 (TaKaRa Bio, Inc., Kusatsu, Japan) were grown in Luria-Bertani (LB) medium supplemented with 30 μM D-biotin. Expression of GroEL/ES molecular chaperone was induced by adding 2 mg/ml L-arabinose when cells reached an optical density at 600 nm of 0.7 to 0.8. About 20 min later, 1 mM IPTG (isopropyl-β-D-thiogalactopyranoside) was added to induce the expression of PCC, followed by additional 16 h at 37°C. Harvested cells were resuspended in 10 mM potassium phosphate buffer (pH 7.0) containing 1 mM dithiothreitol (DTT) and protease inhibitor cocktail (Sigma-Aldrich, St. Louis, MO) and homogenized using an LM-10 or M-110P

microfluidizer (Microfluidics Corp., Westwood, MA). Centrifugation-clarified lysate was purified in two chromatographic steps using Fractogel DEAE resin (Merck Millipore, Billerica, MA) for a capture column, followed by affinity purification using monomeric avidin-agarose (Thermo Fisher Scientific, Waltham, MA). The eluate from the avidin column was desalted on Sephadex G-25 resin (GE Healthcare, Chicago, IL), formulated into 20 mM HEPES (pH 7.4)–100 mM KCl, divided into aliquots, and stored at −80°C. The purification yield of >99% pure PCC from 6 liters of culture was usually between 30 and 100 mg.

Conjugation of purified PCC with TAT peptide. A maleolyl-β-Ala-TAT peptide (Kerafast) targeting accessible cysteine residues was used for conjugation with PCC to prepare TAT-PCC. The reactions were performed overnight in 20 mM HEPES (pH 7.0)–500 mM KCl at a molar ratio for TAT to PCC of 2:1. The unconjugated peptide was removed using Bio-Spin 6 column (Bio-Rad) and formulated into HMS buffer or PBS for import into various systems. Conjugation reaction samples larger than 0.5 ml were processed through a column using Sephadex G-25 resin (GE Healthcare, Chicago, IL). The TAT-PCC conjugate was stable during the freeze-thaw process.

Animals. All animal procedures were approved under the animal protocol B-49417(05)1E by the University of Colorado Denver IACUC, which is an AAALAC-accredited (accreditation 00235), Public Health Service-assured (A3269-01), and USDA-licensed (84-R-0059) institution. We used a hypomorphic mouse model of PA expressing the human PCCA A138T pathogenic mutant on a mouse PCCA-null background (the A138T mouse model) (40, 41). The mice were bred, maintained, and genotyped as described elsewhere (40). Liver PCC activity in A138T mouse was 2.2% of the WT PCC activity. The A138T human cDNA produces 9.4% of the PCC activity in transfected fibroblasts (42). Further, A138T mice have elevated levels of propionylcarnitine, methylcitrate, glycine, alanine, lysine, ammonia, and markers associated with cardiomyopathy, which is similar to levels of these compounds in PA patients.

TAT-PCC in PBS was administered to approximately 12-week-old A138T mice via a single i.p. injection targeting a dose of 20 mg/kg. Two cohorts (A and B) of A138T mice ($n = 4$ each) were used to minimize the blood volume taken from any single mouse, as specified in IACUC protocol. Blood was collected from group A at 0, 2, 4, 8, and 24 h postinjection and from group B at 0, 3, 6, 9 and 24 h postinjection. Age-matched A138T mice injected with PBS ($n = 4$) served as positive controls, which were bled for a sample at 0, 2, 4, 8, and 24 h postinjection. In addition, age-matched WT controls injected with PBS ($n = 4$) served as negative controls, from which blood samples were collected at 0, 3, 6, and 24 h postinjection. A single-use lancet for submandibular bleeding was used for blood collection into Capiject T-MLHG lithium heparin (12.5 IU) tubes with gel (Terumo). Tubes were then centrifuged at 1,200 × *g* for 10 min, followed by collection of plasma into 1.5-ml tubes and storage at −80°C.

Plasma acylcarnitine profile. Plasma concentrations of acylcarnitines were determined by gas chromatography-mass spectrometry (Biochemical Genetics Laboratory of Children's Hospital Colorado). The ratio of propionylcarnitine to acetylcarnitine (C3/C2) was subsequently calculated.

Cell culture. Skin fibroblast cultured cells used for experiments were derived from two patients bearing mutations in either the PCCA or the PCCB gene, as well as from a WT healthy control. The cells were grown in a humidified atmosphere with 5% CO_2 at 37°C and maintained in minimum essential medium supplemented with 15% of Fetal Clone III serum, 100 μM minimal essential medium (MEM), nonessential amino acids, 100 μg/ml penicillin, and 100 μg/ml streptomycin (all from HyClone).

Isolation of mitochondria. Briefly, freshly dissected livers from WT or A138T mice were minced finely before using a motor-driven Teflon and glass Potter-Elvehjem homogenizer (six to nine strokes at 1,000 rpm) in HMS^+ buffer (220 mM D-mannitol, 70 mM sucrose, 2 mM HEPES [pH 7.4], and 0.5 mg/ml bovine serum albumin [BSA]). The first centrifugation of a 15% homogenate in HMS^+ buffer was performed for 1 min at 3,000 × *g* and 4°C using a Beckman Avanti J-25 centrifuge to remove nuclei and cell debris. The supernatant was centrifuged again for 2 min at 18,750 × *g* and 4°C in order to pellet the mitochondria. The resulting pellet was resuspended in HMS^+ buffer and 0.035% digitonin. After 5 min of centrifugation at 18,900 × *g*, the mitochondria were washed three times in HMS buffer (i.e., HMS^+ buffer without BSA) prior to the import studies.

Import of TAT-PCC into isolated mitochondria. The import of TAT-PCC at the desired concentration was performed at 27°C for 30 min. Trypsin was used at a protease/protein ratio of 1:20 (wt/wt) for 5 or 30 min, and the reaction was stopped with soybean trypsin inhibitor at a ratio of 1:1 (wt/wt) with trypsin. The mitochondria were washed in HMS buffer three times, each time centrifuged for 10 min at 18,900 × *g* at 4°C.

Mitochondrial and cell lysates. Mitochondrial or fibroblast pellets were resuspended in fresh lysis buffer (50 mM Tris-HCl [pH 8.0], 1 mM DTT, 1 mM EDTA [pH 8.0], protease inhibitors [Sigma, catalog no. P8340; diluted 1:80]) in a volume three times the size of the pellet. Homogenized mitochondria or fibroblasts were sonicated, and the resulting lysate was clarified by centrifugation (20,000 × *g*, 4°C, 15 min). The protein concentration was determined by a Bradford assay (Thermo-Fisher).

Mitochondrial respiration. The mitochondrial pellet was resuspended in 2.5 ml of the mitochondrial respiration medium MiR05, and oxygen consumption was measured using an Oxygraph-2k (Oroboros Instruments) in 0.5 mM EGTA, 3 mM $MgCl_2 \cdot 6H_2O$, 60 mM potassium lactobionate, 20 mM taurine, 10 mM KH_2PO_4, 20 mM HEPES, 110 mM sucrose, and 1 g/liter fatty acid-free BSA.

PCC activity assay. PCC activity was assayed as described previously with some modifications (3). The reaction mixture contained 50 mM Tris-HCl (pH 8.0), 2 mM ATP, 125 mM KCl, 10 mM $MgCl_2$, 3 mM propionyl-CoA, 0.5 mg/ml BSA, PCC enzyme (0.1 μg of purified PCC or 150 μg of mitochondrial or cell lysate), and 10 mM [^{14}C]bicarbonate (specific activity 2 μCi/μmol) in a final volume of 50 μl, followed by incubation at 37°C for 2 min. The reaction was terminated by adding 50 μl of 10% trichloroacetic acid. The mixture was centrifuged at 13,000 × *g* for 5 min, and 50 μl of the supernatant was dried in a scintillation vial in a heating block at 80°C for 50 min. The dry residue was dissolved in 0.15 ml of H_2O,

and 4 ml of OPTI-Fluor scintillation fluid (Perkin-Elmer Life Sciences) was added. The samples were counted in a Beckman LS-3801 scintillation counter. A blank containing the assay mixture without propionyl-CoA was subtracted. One unit of PCC activity is defined as 1 pmol of product per min at 37°C per mg of protein.

Propionate incorporation assay. The activity of PCC was assessed indirectly by measuring the incorporation of label from [1-^{14}C]propionate into cellular macromolecules (19, 20). Control and patients fibroblasts were grown on six-well plate (Corning). The import of 5 μM TAT-PCC or incubation with PBS was performed at 80% confluence for 1 h at 37°C. Subsequently, the fibroblasts were incubated for 18 h in MEM supplemented with 15% fetal bovine serum (Fetal Clone III) and 100 μM [1-^{14}C]propionate (MD Biochemical), diluted with unlabeled propionate to give a final specific activity of 10 μCi/μmol. At the end of the incubation, the cells were harvested with trypsin, and the cellular macromolecules were precipitated with cold 5% trichloroacetic acid. The precipitated material was dissolved in 0.15 ml of 0.2 N sodium hydroxide, and radioactivity in the precipitate was determined by liquid scintillation counting.

Western blotting. Proteins (50 μg of mitochondrial or cell lysate, 100 ng of purified PCC) were resolved on a SDS–10% PAGE and transferred onto an Immun-Blot polyvinylidene difluoride membrane (Bio-Rad). Western blot analysis was performed with anti-PCCA and anti-PCCB antibodies (both from Abcam) at a 1:1,000 dilution, followed by secondary horseradish peroxidase-conjugated antibody, and proteins were visualized by using chemiluminescent substrate (Super Signal West Pico; Thermo-Fisher).

Import of TAT-PCC into cells. Fibroblast cells were grown in 150-cm^2 flasks. When the cells reached 90% confluence, the medium was removed, followed by a PBS rinse, and replaced with 1 to 10 μM TAT-PCC in PBS. After 1 h incubation at 37°C, the cells were washed with PBS, trypsinized, pelleted, and kept at −80°C until use.

Confocal microscopy. Fibroblast cells were grown in a complete MEM on eight-chamber tissue culture slides (Falcon) to 70% confluence, followed by incubation with 1 μM TAT-PCC for 1.5 h. The cells were then washed with PBS before staining. MitoTracker Red CMXRos was used to stain mitochondria in live cells. Cells were then fixed with 4% formaldehyde for 10 min and permeabilized by methanol. For specific staining, we used anti-PCCA and anti-PCCB primary antibodies with anti-mouse IgG Atto 488-conjugated secondary antibody (Sigma). DAPI staining was used to visualize nuclei. Samples were analyzed using a high-resolution Olympus FV1000 microscope with Software Fluoview for image acquisition.

ACKNOWLEDGMENTS

This study was supported by research grants from Orphan Technologies, Ltd., and the Propionic Acidemia Foundation (to J.P.K.), and T.M. is a recipient of an American Heart Association Scientist Development grant (16SDG30040000). Confocal imaging and genotyping were supported in part by NIH/NCATS Colorado CTSI grant UL1 TR001082.

We declare the following competing financial interest(s): the research was funded by Orphan Technologies, Ltd., a private pharmaceutical company.

We thank Adam Guenzel and Michael A. Barry for providing the A138T mouse model, Marisa Friederich for help with mitochondrial respirations, Sarah Venezia for carrying out the initial fibroblast experiments, and Richard Carrillo for PCC purifications.

The contents of this article are the authors' sole responsibility and do not necessarily represent official NIH views.

REFERENCES

1. Chandler RJ, Venditti CP. 2016. Gene therapy for metabolic diseases. Transl Sci Rare Dis 1:73–89.
2. Fenton WA, Gravel RA, Rosenblatt DS. 2001. Disorders of propionate and methylmalonate metabolism, p 2165–2204. *In* Scriver CR, Beaudet AL, Sly WS, Valle D (ed), The metabolic and molecular bases of inherited disease, 8th ed, vol 2. McGraw-Hill, Inc., New York, NY.
3. Kalousek F, Darigo MD, Rosenberg LE. 1980. Isolation and characterization of propionyl-CoA carboxylase from normal human liver. Evidence for a protomeric tetramer of nonidentical subunits. J Biol Chem 255:60–65.
4. Huang CS, Sadre-Bazzaz K, Shen Y, Deng B, Zhou ZH, Tong L. 2010. Crystal structure of the $\alpha_6\beta_6$ holoenzyme of propionyl-coenzyme A carboxylase. Nature 466:1001–1005. https://doi.org/10.1038/nature09302.
5. Charbit-Henrion F, Lacaille F, McKiernan P, Girard M, de Lonlay P, Valayannopoulos V, Ottolenghi C, Chakrapani A, Preece M, Sharif K, Chardot C, Hubert P, Dupic L. 2015. Early and late complications after liver transplantation for propionic acidemia in children: a two centers study. Am J Transplant 15:786–791. https://doi.org/10.1111/ajt.13027.
6. Frankel AD, Pabo CO. 1988. Cellular uptake of the tat protein from human immunodeficiency virus. Cell 55:1189–1193. https://doi.org/10.1016/0092-8674(88)90263-2.
7. Green M, Loewenstein PM. 1988. Autonomous functional domains of chemically synthesized human immunodeficiency virus tat transactivator protein. Cell 55:1179–1188. https://doi.org/10.1016/0092-8674(88)90262-0.
8. Gohil VM, Greenberg ML. 2009. Mitochondrial membrane biogenesis: phospholipids and proteins go hand in hand. J Cell Biol 184:469–472. https://doi.org/10.1083/jcb.200901127.
9. Schmidt O, Pfanner N, Meisinger C. 2010. Mitochondrial protein import: from proteomics to functional mechanisms. Nat Rev Mol Cell Biol 11:655–667. https://doi.org/10.1038/nrm2959.
10. Neupert W, Herrmann JM. 2007. Translocation of proteins into mitochondria. Annu Rev Biochem 76:723–749. https://doi.org/10.1146/annurev.biochem.76.052705.163409.
11. Hawlitschek G, Schneider H, Schmidt B, Tropschug M, Hartl FU, Neupert W. 1988. Mitochondrial protein import: identification of processing peptidase and of PEP, a processing enhancing protein. Cell 53:795–806. https://doi.org/10.1016/0092-8674(88)90096-7.

12. Gakh O, Cavadini P, Isaya G. 2002. Mitochondrial processing peptidases. Biochim Biophys Acta 1592:63–77. https://doi.org/10.1016/S0167-4889(02)00265-3.
13. Del Gaizo V, Payne RM. 2003. A novel TAT-mitochondrial signal sequence fusion protein is processed, stays in mitochondria, and crosses the placenta. Mol Ther 7:720–730. https://doi.org/10.1016/S1525-0016(03)00130-8.
14. Vyas PM, Payne RM. 2008. TAT opens the door. Mol Ther 16:647–648. https://doi.org/10.1038/mt.2008.24.
15. Rapoport M, Saada A, Elpeleg O, Lorberboum-Galski H. 2008. TAT-mediated delivery of LAD restores pyruvate dehydrogenase complex activity in the mitochondria of patients with LAD deficiency. Mol Ther 16:691–697. https://doi.org/10.1038/mt.2008.4.
16. Marcus D, Lichtenstein M, Saada A, Lorberboum-Galski H. 2013. Replacement of the C6ORF66 assembly factor (NDUFAF4) restores complex I activity in patient cells. Mol Med 19:124–134. https://doi.org/10.2119/molmed.2012.00343.
17. Vyas PM, Tomamichel WJ, Pride PM, Babbey CM, Wang Q, Mercier J, Martin EM, Payne RM. 2012. A TAT-frataxin fusion protein increases lifespan and cardiac function in a conditional Friedreich's ataxia mouse model. Hum Mol Genet 21:1230–1247. https://doi.org/10.1093/hmg/ddr554.
18. Darvish-Damavandi M, Ho HK, Kang TS. 2016. Towards the development of an enzyme replacement therapy for the metabolic disorder propionic acidemia. Mol Genet Metab Rep 8:51–60. https://doi.org/10.1016/j.ymgmr.2016.06.009.
19. Gravel RA, Lam KF, Scully KJ, Hsia Y. 1977. Genetic complementation of propionyl-CoA carboxylase deficiency in cultured human fibroblasts. Am J Hum Genet 29:378–388.
20. Watkins D, Matiaszuk N, Rosenblatt DS. 2000. Complementation studies in the *cblA* class of inborn error of cobalamin metabolism: evidence for interallelic complementation and for a new complementation class (*cblH*). J Med Genet 37:510–513. https://doi.org/10.1136/jmg.37.7.510.
21. Hill HZ, Goodman SI. 1974. Detection of inborn errors of metabolism. II. Defects in propionic acid metabolism. Clin Genet 6:73–78.
22. Palm-Apergi C, Lonn P, Dowdy SF. 2012. Do cell-penetrating peptides actually "penetrate" cellular membranes? Mol Ther 20:695–697. https://doi.org/10.1038/mt.2012.40.
23. Madani F, Lindberg S, Langel U, Futaki S, Graslund A. 2011. Mechanisms of cellular uptake of cell-penetrating peptides. J Biophys 2011:414729. https://doi.org/10.1155/2011/414729.
24. Raagel H, Saalik P, Pooga M. 2010. Peptide-mediated protein delivery-which pathways are penetrable? Biochim Biophys Acta 1798:2240–2248. https://doi.org/10.1016/j.bbamem.2010.02.013.
25. Rayapureddi JP, Tomamichel WJ, Walton ST, Payne RM. 2010. TAT fusion protein transduction into isolated mitochondria is accelerated by sodium channel inhibitors. Biochemistry 49:9470–9479. https://doi.org/10.1021/bi101057v.
26. Fuerst JA, Sagulenko E. 2010. Protein uptake by bacteria: an endocytosis-like process in the planctomycete *Gemmata obscuriglobus*. Commun Integr Biol 3:572–575. https://doi.org/10.4161/cib.3.6.13061.
27. Rapoport M, Salman L, Sabag O, Patel MS, Lorberboum-Galski H. 2011. Successful TAT-mediated enzyme replacement therapy in a mouse model of mitochondrial E3 deficiency. J Mol Med 89:161–170. https://doi.org/10.1007/s00109-010-0693-3.
28. Schiffmann R, Murray GJ, Treco D, Daniel P, Sellos-Moura M, Myers M, Quirk JM, Zirzow GC, Borowski M, Loveday K, Anderson T, Gillespie F, Oliver KL, Jeffries NO, Doo E, Liang TJ, Kreps C, Gunter K, Frei K, Crutchfield K, Selden RF, Brady RO. 2000. Infusion of alpha-galactosidase A reduces tissue globotriaosylceramide storage in patients with Fabry disease. Proc Natl Acad Sci U S A 97:365–370. https://doi.org/10.1073/pnas.97.1.365.
29. Amalfitano A, Bengur AR, Morse RP, Majure JM, Case LE, Veerling DL, Mackey J, Kishnani P, Smith W, McVie-Wylie A, Sullivan JA, Hoganson GE, Phillips JA, III, Schaefer GB, Charrow J, Ware RE, Bossen EH, Chen YT. 2001. Recombinant human acid alpha-glucosidase enzyme therapy for infantile glycogen storage disease type II: results of a phase I/II clinical trial. Genet Med 3:132–138. https://doi.org/10.1097/00125817-200103000-00007.
30. Bublil EM, Majtan T, Park I, Carrillo RS, Hulkova H, Krijt J, Kozich V, Kraus JP. 2016. Enzyme replacement with PEGylated cystathionine beta-synthase ameliorates homocystinuria in murine model. J Clin Invest 126:2372–2384. https://doi.org/10.1172/JCI85396.
31. Kakkis ED, Muenzer J, Tiller GE, Waber L, Belmont J, Passage M, Izykowski B, Phillips J, Doroshow R, Walot I, Hoft R, Neufeld EF. 2001. Enzyme-replacement therapy in mucopolysaccharidosis. I N Engl J Med 344:182–188. https://doi.org/10.1056/NEJM200101183440304.
32. Eng CM, Guffon N, Wilcox WR, Germain DP, Lee P, Waldek S, Caplan L, Linthorst GE, Desnick RJ, International Collaborative Fabry Disease Study Group. 2001. Safety and efficacy of recombinant human alpha-galactosidase A replacement therapy in Fabry's disease. N Engl J Med 345:9–16. https://doi.org/10.1056/NEJM200107053450102.
33. Connock M, Burls A, Frew E, Fry-Smith A, Juarez-Garcia A, McCabe C, Wailoo A, Abrams K, Cooper N, Sutton A, O'Hagan A, Moore D. 2006. The clinical effectiveness and cost-effectiveness of enzyme replacement therapy for Gaucher's disease: a systematic review. Health Technol Assess 10:1–136. https://doi.org/10.3310/hta10200.
34. Wraith JE, Clarke LA, Beck M, Kolodny EH, Pastores GM, Muenzer J, Rapoport DM, Berger KI, Swiedler SJ, Kakkis ED, Braakman T, Chadbourne E, Walton-Bowen K, Cox GF. 2004. Enzyme replacement therapy for mucopolysaccharidosis I: a randomized, double-blinded, placebo-controlled, multinational study of recombinant human alpha-L-iduronidase (laronidase). J Pediatr 144:581–588. https://doi.org/10.1016/j.jpeds.2004.01.046.
35. Strisciuglio P, Concolino D. 2014. New strategies for the treatment of phenylketonuria (PKU). Metabolites 4:1007–1017. https://doi.org/10.3390/metabo4041007.
36. Sarkissian CN, Kang TS, Gamez A, Scriver CR, Stevens RC. 2011. Evaluation of orally administered PEGylated phenylalanine ammonia lyase in mice for the treatment of phenylketonuria. Mol Genet Metab 104:249–254. https://doi.org/10.1016/j.ymgme.2011.06.016.
37. Kang TS, Wang L, Sarkissian CN, Gamez A, Scriver CR, Stevens RC. 2010. Converting an injectable protein therapeutic into an oral form: phenylalanine ammonia lyase for phenylketonuria. Mol Genet Metab 99:4–9. https://doi.org/10.1016/j.ymgme.2009.09.002.
38. Harmatz P, Whitley CB, Waber L, Pais R, Steiner R, Plecko B, Kaplan P, Simon J, Butensky E, Hopwood JJ. 2004. Enzyme replacement therapy in mucopolysaccharidosis VI (Maroteaux-Lamy syndrome). J Pediatr 144:574–580. https://doi.org/10.1016/j.jpeds.2004.03.018.
39. Kelson TL, Ohura T, Kraus JP. 1996. Chaperonin-mediated assembly of wild-type and mutant subunits of human propionyl-CoA carboxylase expressed in *Escherichia coli*. Hum Mol Genet 5:331–337. https://doi.org/10.1093/hmg/5.3.331.
40. Guenzel AJ, Hofherr SE, Hillestad M, Barry M, Weaver E, Venezia S, Kraus JP, Matern D, Barry MA. 2013. Generation of a hypomorphic model of propionic acidemia amenable to gene therapy testing. Mol Ther 21:1316–1323. https://doi.org/10.1038/mt.2013.68.
41. Guenzel AJ, Collard R, Kraus JP, Matern D, Barry MA. 2015. Long-term sex-biased correction of circulating propionic acidemia disease markers by adeno-associated virus vectors. Hum Gene Ther 26:153–160. https://doi.org/10.1089/hum.2014.126.
42. Clavero S, Martinez MA, Perez B, Perez-Cerda C, Ugarte M, Desviat LR. 2002. Functional characterization of PCCA mutations causing propionic acidemia. Biochim Biophys Acta 1588:119–125. https://doi.org/10.1016/S0925-4439(02)00155-2.
43. Jiang H, Rao KS, Yee VC, Kraus JP. 2005. Characterization of four variant forms of human propionyl-CoA carboxylase expressed in Escherichia coli. J Biol Chem 280:27719–27727. https://doi.org/10.1074/jbc.M413281200.